

L.C. CASPER<sup>1,✉</sup>  
H.M.J. BASTIAENS<sup>1</sup>  
P.J.M. PETERS<sup>1</sup>  
K.-J. BOLLER<sup>1</sup>  
R.M. HOFSTRA<sup>2</sup>

## Long-pulse KrCl laser with a high discharge quality

<sup>1</sup> Faculty of Science and Technology, University of Twente, P.O. Box 217, 7500 AE Enschede, The Netherlands

<sup>2</sup> Nederlands Centrum voor Laser Research (NCLR) B.V., P.O. Box 2662, 7500 CR Enschede, The Netherlands

Received: 16 January 2007/Revised version: 28 February 2007  
Published online: 25 April 2007 • © Springer-Verlag 2007

**ABSTRACT** The discharge quality and optimum pump parameters of a long-pulse high-pressure gas discharge excited KrCl laser are investigated. A three-electrode prepulse–mainpulse excitation circuit is employed as pump source. The discharge volume contains a gas mixture of HCl/Kr/Ne operated at a total pressure of up to 5 bar. For a plane–plane resonator, the divergence of both output laser beams is measured. A low beam divergence of less than 1 mrad is measured as a result of the very high discharge homogeneity. A maximum laser pulse duration of 150 ns (FWHM) is achieved for a pump duration of 270 ns (FWHM) and a power density of  $340 \text{ kW cm}^{-3}$ . Pumping the discharge under optimum conditions employing a stable resonator results in a maximum specific energy of  $0.45 \text{ J/l}$  with a laser pulse duration of 117 ns and an efficiency of 0.63% based on the deposited energy.

**PACS** 42.55.Lt; 52.25.-b; 52.59.Ye

### 1 Introduction

High-pressure gas-discharge pumped rare-gas halide excimer lasers are sources of very powerful ultraviolet (UV) radiation. The wavelength range covered and the high pulse energies have made excimer lasers an extensively used tool for applications in science, industry and also in medicine [1, 2]. Gas discharge pumping opened the way to UV-lasers with pulse repetition rates up to several kHz with output powers up to the kW-level. However, excimer lasers pumped by a simple charge-transfer circuit [3, 4] are restricted to low efficiencies and short pulse durations of only a few tens of nanoseconds. Voltage matching between the storage capacitance used to pump the laser and the discharge steady-state voltage is hardly achievable with such circuits. The discharge current tends to oscillate under these conditions. Discharge instabilities grow rapidly due to the voltage mismatching and the current oscillation. The beam quality of these lasers is poor, as the required time to build up a beam with a low divergence is longer than the stability time of the discharge.

An important step to increase the efficiency and pulse duration of excimer lasers has been the development of

the prepulse–mainpulse excitation technique [5, 6]. The prepulse, a very fast rising high-voltage pulse, is applied to the discharge electrodes within a few nanoseconds after preionization to initiate the discharge homogeneously. A low-impedance circuit generates the mainpulse in order to sustain the discharge and to pump the laser. The mainpulse voltage can be chosen independently from the prepulse voltage. Therefore, matching between the sustaining voltage and the steady-state voltage can be realized. As a result, this excitation technique leads to an optimization of the pump efficiency as the voltage matching is possible and current ringing can be avoided. The discharge stability improves considerably and leads to an extension of the laser pulse duration. In the case of XeCl lasers (308 nm), laser pulse durations of several hundreds of nanoseconds with efficiencies up to 5% have been realized [7, 8] and raised strong interest in science and industry. XeCl lasers were subject to intense experimental and theoretical studies leading to the demonstration of nearly diffraction limited laser beams [9]. In particular KrCl lasers (222 nm) were found to be very interesting for industrial applications, due to the prospect of a shorter wavelength and a higher photon energy compared to XeCl. It was expected that long laser pulse durations and a high beam quality could be achieved with KrCl lasers as well due to the use of the same halogen donor. However, it has been found experimentally that the discharge stability and efficiency of KrCl lasers is lower compared to XeCl. Although KrCl lasers operated with high power densities of  $5 \text{ MW cm}^{-3}$  have reached efficiencies of up to 2.6%, pulse durations have been limited to only a few tens of nanoseconds [10]. Long laser pulse durations in KrCl have been demonstrated first by Hueber et al. comprising a compact prepulse–mainpulse excitation scheme [11]. The laser pulse duration could be extended to 135 ns when it has been pumped with a power density of  $700 \text{ kW cm}^{-3}$ . To separate electrically the mainpulse from the prepulse, the excitation circuit has been equipped with a saturable magnetic inductor switch [5]. These switches are commonly used, as they are reliable and possess a long lifetime. A serious drawback is nevertheless the high rest self-inductance after switching. This causes the dissipation of a part of the pump energy, reducing the overall laser efficiency. Furthermore, the switch inductance reduces the achievable pump power and in-

✉ Fax: +31 53 4891102, E-mail: l.c.casper@tnw.utwente.nl

creases the discharge current rise time. The latter is assumed to reduce the discharge stability [12].

To overcome these limitations set by magnetic switches, we employ a three-electrode discharge circuit [13–15] to pump a high-pressure KrCl laser. In this laser, two discharge volumes are formed by using three electrodes. The prepulse circuit is connected to the intermediate electrode, while the mainpulse circuit is connected to the outer electrodes. The electrode gaps separate the mainpulse from the prepulse. Therefore, no additional elements are required and the circuit inductance can be minimized to the intrinsic rest self-inductance given by the laser geometry. Borovkov et al. have demonstrated a KrCl three-electrode laser with an efficiency of 0.5% and a laser pulse energy of 0.25 J [15]. However, no information about the power deposition, the laser pulse duration or the discharge homogeneity has been given. We note that so far, no other studies have reported the quality of the discharge in long-pulses KrCl excimer lasers.

This paper presents the first studies on the discharge quality of a high-pressure gas discharge pumped, long-pulse KrCl laser. Particularly, we conclude from measurements of the divergence of the laser beams emerging from both volumes that the discharge quality is comparably to long-pulse XeCl lasers with a high discharge homogeneity. A low divergence of less than 1 mrad is measured for both laser beams independently. Long-optical pulses up to 150 ns (FWHM) with pulse energies of 0.27 J/l are generated when pumped with a pump power density of  $340 \text{ kW cm}^{-3}$ . Additionally, studies on different resonator configurations under the same pump conditions reveal output energies of up to 0.45 J/l with pulse durations of 117 ns.

## 2 Experimental setup

A three-electrode discharge cell and electric pump circuit was designed and built to sustain high-pressure discharges in KrCl-excimer gas mixtures. The insulator material, used for the laser vessel is made of a halogen resistant polymer. Typically, high-pressure Kr/HCl/Ne mixtures with gas pressures up to 5 bar are used during the experiments. A cryogenic gas purifier circulates the gas through the discharge volume. The HCl partial pressure is controlled by the gas purifier. The discharge cell is sealed off from ambient air using anti-reflection coated windows (fused silica). View ports in the side of the laser chamber allow the observation of the discharge development also in the transverse direction.

Figure 1 shows a schematic overview of the electric circuit and the three-electrode discharge cell. All electrodes are made of nickel-coated aluminum. The middle-electrode is a 1 mm

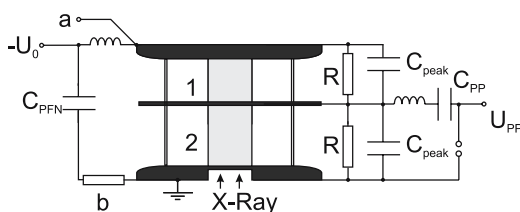


**FIGURE 1** Electric pumping scheme of the three-electrode laser.  $C_{\text{PFN}} = 800 \text{ nF}$ ,  $C_{\text{pp}} = 3.6 \text{ nF}$ ,  $C_{\text{peak}} = 3.4 \text{ nF}$ . a: Voltage probe position; b: current probe position

thick plate placed between the anode and cathode, thus forming two discharge volumes (labeled as 1 and 2 in Fig. 1). The inter-electrode distances are  $d_1 = 1.7 \text{ cm}$  (volume 1) and  $d_2 = 2.0 \text{ cm}$  (volume 2). The discharge volumes are preionized using a fast rising ( $\tau_{\text{rise}} = 20 \text{ ns}$ ) X-ray pulse. The radiation penetrates the discharge cell through a rectangular window in the lower electrode. The cross section of this window defines the preionization area in both volumes. The volumes are preionized over a length of 80 cm and a maximum width of 2 cm, giving a maximum total discharge volume of  $592 \text{ cm}^3$ .

The prepulse circuit consists of a single capacitor of  $C_{\text{pp}} = 3.6 \text{ nF}$  that is mounted on an  $\text{N}_2$ -pressurized spark gap. A Marx Generator generates a high-voltage pulse to charge  $C_{\text{pp}}$  to voltages up to 39 kV. The spark gap is configured such that it triggers spontaneously as  $C_{\text{pp}}$  is fully charged. Careful adjustment of the spark-gap pressure and voltage leads to a time jitter of less than 25 ns with respect to the X-ray pulse. After triggering the spark gap, the charge is transferred to the total peaking capacitance  $2C_{\text{peak}} = 6.8 \text{ nF}$ . In this configuration, a prepulse with negative polarity and a rise time of 32 ns is generated. The application of the prepulse leads to the breakdown in both volumes with volume 2 starting first and being followed by volume 1. Thereafter, the low-impedance pulse forming network (PFN) sustains the discharges in both volumes. The PFN consists of seven rows of 26 ceramic capacitors each with a total capacitance of 800 nF. The PFN is pulse-charged to a maximum voltage of 15 kV with a negative polarity. A resistive voltage-divider probe located at position a, as shown in Fig. 1, measures the anode–cathode voltage. A shunt-resistor probe in the current return loop to the PFN (position b in Fig. 1) measures the discharge current. The deposited electric power  $P(t) = U(t) \cdot I(t)$ , is calculated from the measured discharge current  $I(t)$  and anode–cathode voltage  $U(t)$ . The latter is corrected for inductive effects ( $L_{\text{head}} dI/dt$ ) arising from the laser head self-inductance  $L_{\text{head}}$ .

The discharge quality is investigated by measuring the divergence of the laser beams emerging from both volumes when equipped with a plane–plane resonator, as shown in Fig. 2a. The laser beam generated in such a resonator reflects very strongly the spatial homogeneity of the gain medium. The amplification of photons emitted parallel to the optical axis is higher than for photons emitted in a nonparallel di-

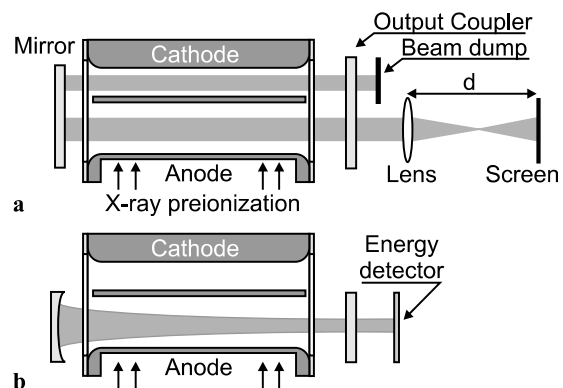


**FIGURE 2** Resonator configurations of the three-electrode KrCl discharge laser. (a) Plane–plane resonator used to measure the beam propagation, (b) concave–plane resonator to optimize the output energy

rection. This causes photons mostly to traverse the discharge region within a small sub-volume of the gain medium parallel to the optical axis. As an example, in the near field intensity distribution of long-pulse XeCl laser beams, discharge-inhomogeneities, e.g., streamers, have been observed in the burn pattern [16]. Furthermore, after focusing the beam with a lens, the beam divergence can be used as a relative measure of the discharge quality when compared to lasers with known discharge quality and beam divergence. Laser beams generated in a discharge with a poor spatial homogeneity have a very large beam divergence compared to laser beams generated in discharges with a high spatial homogeneity.

In this measurement scheme, an output coupler with a reflection coefficient of  $R_{OC} = 0.9$  is used in combination with a highly-reflecting mirror ( $R > 0.999$ ). The resonator length is  $L = 1.5$  m while the active region of the laser has a length of  $L_d = 0.8$  m. The beams are focused separately on thermo-sensitive paper using a lens with a focal length of 1 m. The beam profile is inspected from the beam imprint on the paper at various distances from the lens along the optical axis, thereby giving a first impression of the discharge homogeneity. Furthermore, the maximum extractable output is determined. For this, an external plane-concave resonator employing volume 2 as oscillator is built, as shown in Fig. 2b. To enable reaching the laser threshold at a variety of pumping conditions, a stable, low-loss resonator is chosen. Reflection coefficients of  $R = 0.5, 0.7, 0.8, 0.9$  of the output coupler are used in combination with a highly-reflecting ( $R > 0.999$ ) curved mirror ( $r_c = 5$  m). The cross section of the laser beams, as given by the preionized volume is  $2.0 \times 1.7$  cm<sup>2</sup> for the upper volume and  $2.0 \times 2.0$  cm<sup>2</sup> for the lower volume.

The temporal shape of the laser pulse is measured using a fast photodiode (rise time  $< 2$  ns) behind an UV bandpass filter ( $\lambda_c = 214 \pm 12$  nm). The laser pulse energy is measured using a calibrated pyro-electric detector. All experiments are carried out as single shot measurements.

### 3 Experimental results and discussion

#### 3.1 Discharge quality

In a first experiment, the KrCl laser is characterized with the plane-plane resonator. For this, the pulse energy and laser pulse duration are measured. A HCl/Kr/Ne gas mixture is used with partial pressures of (1/90/3210) mbar. In order to measure the dependence of the pulse duration and energy on the pump power density, the PFN charging voltage ( $U_{PFN}$ ) is increased from 10 to 12 kV. This way, the power deposition changes from  $220$  kW cm<sup>-3</sup> to  $350$  kW cm<sup>-3</sup>. The pump pulse duration, as given by the PFN circuit, remains constant at 270 ns (FWHM). The results of the measurements are shown in Fig. 3. The pulse energy of both volumes increases from 69 mJ for 10 kV to 92 mJ for a charging voltage of 12 kV, while the laser pulse duration remains nearly constant at 137 ns.

In a next experiment employing the plane-plane resonator, the beam divergence of both laser beams is investigated. The measurement is performed for each beam separately by blocking one of the beams at a time (behind the outcoupler). A lens with a focal length of 1 m is used to focus the remaining beam on thermo-sensitive paper. The spot size is measured from the

burn pattern on the paper. The measurement is repeated at various positions along the optical axis close to and in the focal plane of the lens. The measured spot size  $w$  plotted as function of the distance  $d$  to the lens is shown in Fig. 4a for the upper volume and in Fig. 4b for the lower volume. Shown is the spot size measured in the horizontal (filled symbol)

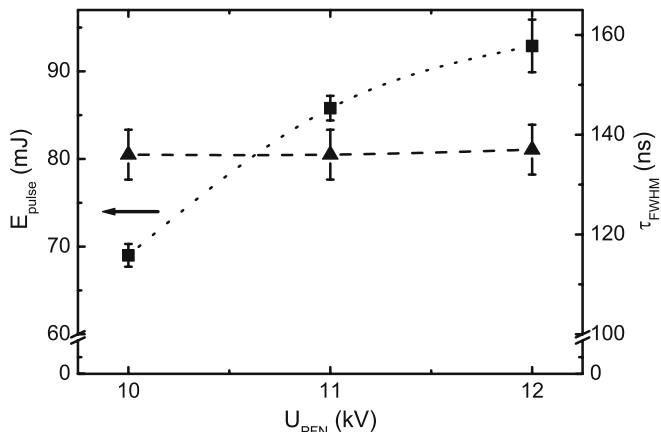


FIGURE 3 Laser pulse duration  $\tau_{FWHM}$  and pulse energy  $E_{pulse}$  for a plane-plane resonator as function of the PFN charging voltage  $U_{PFN}$ . Output coupler reflectivity  $R_{OC} = 0.9$ . Gas composition: HCl/Kr/Ne mixture of (1/90/3210) mbar

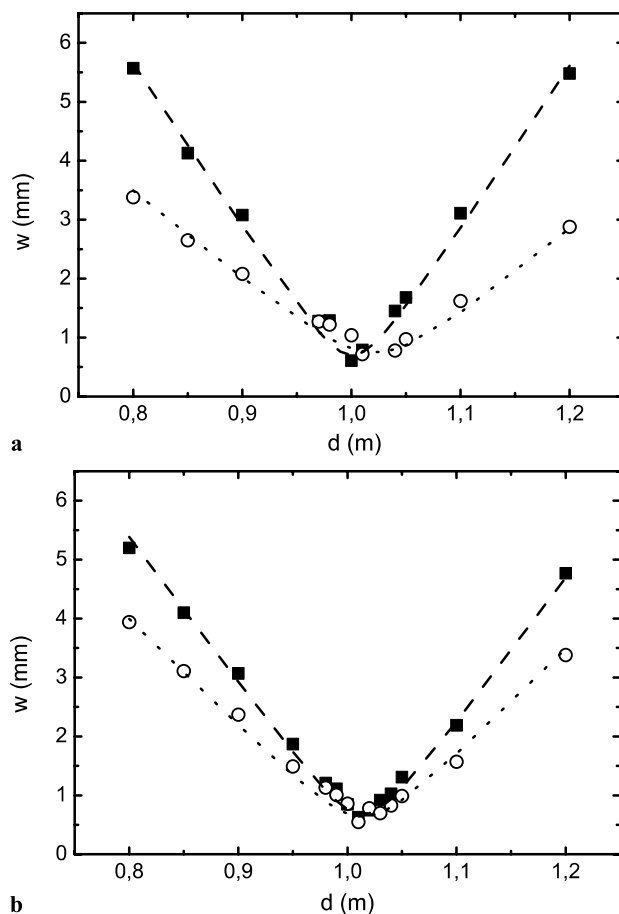
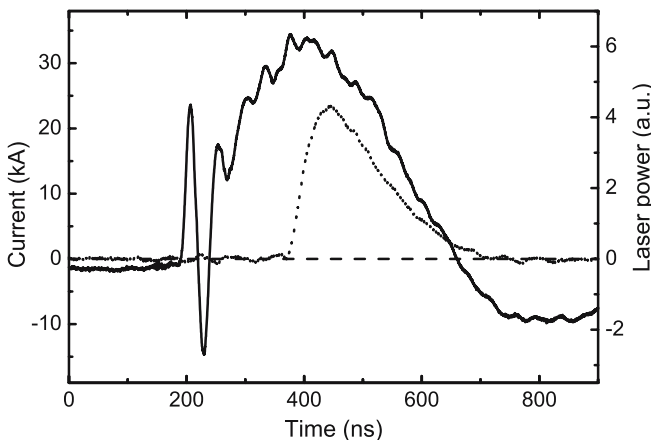


FIGURE 4 Beam waist  $w$  of the laser beam emerging from (a) the upper volume and (b) the lower volume measured as function of the distance  $d$  to the focusing lens ( $f = 1$  m). ■ – horizontal axis, ○ – vertical axis. Lines are drawn to guide the eye

and vertical plane (open symbol), respectively. A beam waist of  $w_{0,x} = 800 \mu\text{m}$  for the horizontal and  $w_{0,y} = 750 \mu\text{m}$  for the vertical plane is measured for the lower volume. For the upper volume, a similar result is found with  $w_{0,x} = 700 \mu\text{m}$  and  $w_{0,y} = 750 \mu\text{m}$ . From these plots, the beam divergence is calculated for the lower volume to be  $\Theta_x = 0.8 \text{ mrad}$  and  $\Theta_y = 0.6 \text{ mrad}$ . For the upper volume  $\Theta_x = 1.0 \text{ mrad}$  and  $\Theta_y = 0.5 \text{ mrad}$  are obtained.

These results are compared with the measured beam divergence of a long-pulse XeCl laser [17, 18] with comparable discharge and resonator dimensions, because that laser has shown an excellent discharge quality. A beam divergence of 3 mrad has been reported for that XeCl laser when equipped with a plane–plane resonator, generating laser beams with a comparable beam cross section [16, 17]. On the one hand, the beam divergence is approximately proportional to the wavelength  $\lambda$ , thus principally a lower beam divergence may be expected for KrCl lasers compared to XeCl lasers. On the other hand, strong inhomogeneities in the gain medium due to the formation of streamers or even a constriction of the discharge due to arcing would result in a higher beam divergence. The measured beam divergence of the KrCl laser is found to be lower by a factor of three compared to the named XeCl laser. We conclude from this that the KrCl laser beam indeed builds up in a very homogeneous discharge. Consistent with this, the discharge appears homogeneous in a visual inspection through the transverse windows of the discharge cell. Also supporting our conclusion of a very homogeneous discharge, we find the shot-to-shot variation of the pulse energy, as indicated by the error bars in Fig. 3, to be very low with a value of below 3% for loading voltages up to 11 kV.

Additionally measured is the temporal evolution of the laser pulse with respect to the discharge current, as it shows the stage of the discharge the pulse is traversing the gain medium. A typical example for the measured discharge current and laser pulse is shown in Fig. 5 for a gas mixture containing  $p_{\text{HCl}} = 1 \text{ mbar}$ ,  $p_{\text{Kr}} = 90 \text{ mbar}$  and  $p_{\text{Ne}} = 3.2 \text{ bar}$ . The PFN is charged to a voltage of 12 kV. The slightly negative current (solid line) during the first 180 ns indicates the charging of the prepulse capacitance. The prepulse is ap-



**FIGURE 5** Typical waveform of the discharge current (*solid*) and laser pulse (*dotted*) measured for a gas pressure of  $p_{\text{Ne}} = 3.2 \text{ bar}$ ,  $p_{\text{Kr}} = 90 \text{ mbar}$  and  $p_{\text{HCl}} = 1 \text{ mbar}$ . The PFN is charged to a voltage of 12 kV. The resonator consists of plane mirrors with reflection coefficients of  $R \approx 1$  and  $R_{\text{OC}} = 0.9$

plied to the middle-electrode in order to initiate a discharge in both volumes consecutively. As the first volume breaks down, the current rises very sharply to 22 kA ( $t = 200 \text{ ns}$ ) and decreases thereafter to  $-15 \text{ kA}$ . During this time, the discharge in the second volume is initiated, as the voltage on the middle-electrode reverses and rises until the breakdown threshold is reached. After the discharge is established in both volumes ( $t \approx 220 \text{ ns}$ ), the current rises to a peak value of 32 kA in the following 150 ns (defined as 10%–90% increase of the peak value). The peak power deposition is calculated to be  $340 \text{ kW cm}^{-3}$ . Such a power deposition is relatively low for a KrCl laser and comparable to long-pulse XeCl lasers. At  $t = 650 \text{ ns}$ , the discharge current reduces and reverses, as the PFN charging voltage was not fully matched to the discharge voltage. As shown in Fig. 5, the laser pulse (*dotted line*) appears at  $t = 380 \text{ ns}$  as the peak current is reached and shows that the laser pulse build up during the first 150 ns of the discharge. The pulse reaches a duration (FWHM) of 137 ns and ends with the end of the pump pulse. Therefore, the laser pulse used to measure the beam divergence traverses the gain medium mainly during the second half of the discharge.

### 3.2 Optimizing for maximum output

To determine the optimum gas pressure that provides the highest output energies and longest pulse duration, both laser parameters are measured for different buffer gas and rare-gas pressures for the lower discharge volume. As shown in Fig. 2b, we use the concave–plane resonator for this experiment. It provided higher output energies compared to the plane–plane resonator when equipped with an output coupler transmitting 10%. A high reflecting mirror with a radius of curvature of 5 m is centered on the optical axis of the larger discharge volume. In these experiments, the reduced field  $E/p$  is kept constant at a value of  $\approx 0.37 \text{ kV cm}^{-1} \text{ bar}^{-1}$ . For this, the PFN charging voltage is increased with the gas pressure. Furthermore, a constant HCl partial pressure of 1 mbar is used. We found in a parametric study that this pressure provides in our laser the longest pulse durations with high output energies when compared to other HCl partial pressures.

The laser pulse energy is measured as a function of the Ne partial pressure, as shown in Fig. 6. The measurements are carried out with gas mixtures containing either  $p_{\text{Kr}} = 90 \text{ mbar}$  or  $p_{\text{Kr}} = 130 \text{ mbar}$ . We find a peak pulse energy of 85 mJ for a Kr partial pressure of 90 mbar and  $p_{\text{Ne}} = 4.3 \text{ bar}$ . Increasing  $p_{\text{Kr}}$  to 130 mbar resulted in a shift of the optimum Ne pressure to a lower value of around 3.8 bar. With a krypton partial pressure below 60 mbar, no laser action is observed.

The laser pulse durations observed for different Ne pressures are presented in Fig. 7. For a Kr partial pressure of 90 mbar, the maximum pulse duration of 152 ns is obtained at a Ne pressure of 3.3 bar and decreases to 145 ns beyond this pressure. It can be seen that the pulse duration changes only by 5% in the investigated pressure range, while the energy changes by about 80% and therefore, mainly the peak power increases with the pressure. For a Kr partial pressure of 130 mbar, we find the peak pulse duration of 148 ns for a Ne pressure of 3.3 bar.



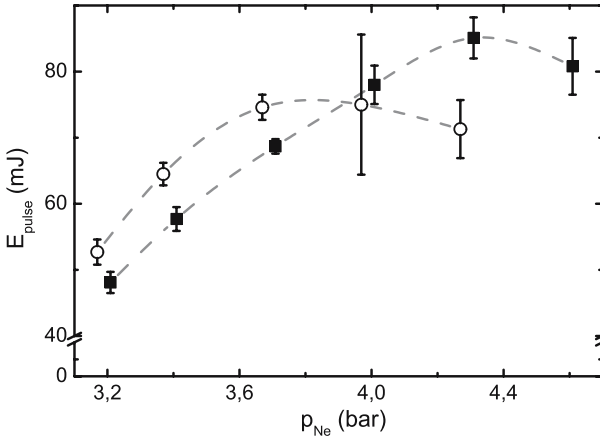


**FIGURE 6** Laser pulse energy  $E_{\text{pulse}}$  as function of the Ne pressure  $p_{\text{Ne}}$  and for two different Kr partial pressures. ■ –  $p_{\text{Kr}} = 90$  mbar, ○ –  $p_{\text{Kr}} = 130$  mbar. Output coupler reflectivity  $R_{\text{OC}} = 0.9$  and radius of curvature of the total reflector ( $R > 0.999$ ) with  $r_c = 5$  m

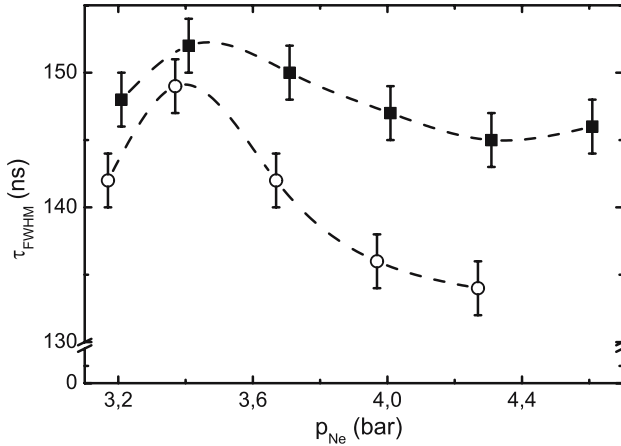
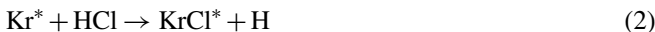


**FIGURE 7** Laser pulse duration  $\tau_{\text{FWHM}}$  as function of the Ne pressure  $p_{\text{Ne}}$  and for two different Kr partial pressures. ■ –  $p_{\text{Kr}} = 90$  mbar, ○ –  $p_{\text{Kr}} = 130$  mbar. Output coupler reflectivity  $R_{\text{OC}} = 0.9$  and radius of curvature of the reflector ( $R > 0.999$ )  $r_c = 5$  m

In the following, an interpretation of the obtained results based on a qualitative discussion of the basic chemical reactions in the discharge is given. The optimum working pressure of the laser, as determined by the pulse duration and output energy, is given by the balance of the production and loss of KrCl molecules. The initial enhanced pulse energy employing a higher Kr partial pressure is assumed to be the result of a faster formation of KrCl, as the initial  $\text{Kr}^+$  density is higher:



Therefore, a higher electron density due to the additional ionization of excited Kr atoms is expected. The consumption of HCl and  $\text{HCl}(v)$  increases with the higher electron density as a consequence of the high electron attachment rate [19] for the low  $E/p$  values used to generate long optical pulses. The harpooning reaction



is only of minor importance in the formation of KrCl, as Peet et al. [20] pointed out. A contribution of 5% to the KrCl

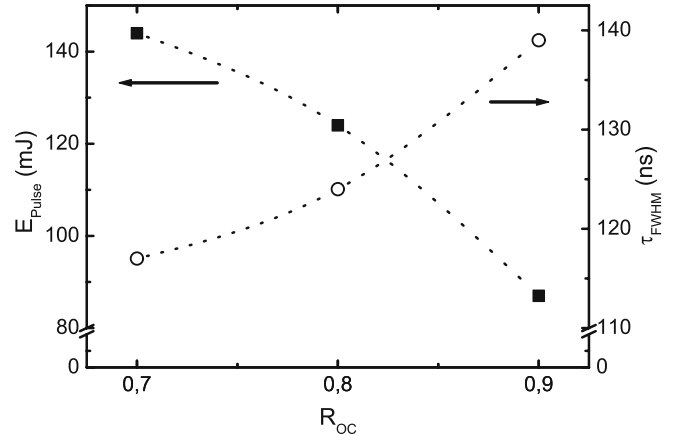


**FIGURE 8** Laser pulse energy (■) and pulse duration (○) as function of the output coupler reflectivity  $R_{\text{OC}}$ . Gas mixture: HCl/Kr/Ne with partial pressures of (1/90/4310) mbar

formation was determined using a short pulse laser pumped with power densities of several  $\text{MW cm}^{-3}$ . It looks therefore advantageous, to increase the HCl partial pressure to compensate the consumption. Indeed, adding HCl to the gas mixture has been observed to increase the pulse energy but also to reduce the pulse duration. The  $\text{KrCl}^*$ -density is expected to increase as more  $\text{Cl}^-$ -ions are present in the discharge. Nonetheless, increasing the Ne pressure above the optimum pressure reduces the upper laser state population due to enhanced quenching processes of  $\text{KrCl}^*$  involving the rare-gas and buffer gas, e.g.,



From this we conclude that the laser performance is determined by the halogen consumption and the quenching processes taking place in the gas discharge.

Measurements on the resonator output coupler transmission to achieve the highest pulse energy are carried out, using the previously determined optimum gas composition. These measurements employ the lower discharge volume as laser medium. The output coupler reflectivity is reduced from  $R_{\text{OC}} = 0.9$  to 0.8 and 0.7. The gas cell is filled with the gas mixture of HCl/Kr/Ne = (1/90/4310) mbar while the PFN is charged to a voltage of 11.7 kV.

The measured pulse energies and durations as a function of the output coupler reflectivity are shown in Fig. 8. A pulse energy (filled symbol) of 85 mJ is measured with the 90% reflectivity used. With this resonator, a laser pulse duration (open symbol) of 139 ns (FWHM) is observed. The energy increases to 144 mJ as  $R_{\text{OC}}$  is reduced to 70%. This energy corresponds to a specific pulse energy of 0.45 J/l and a laser efficiency of 0.63% based on the deposited energy in the volume. For this output coupler reflectivity, the laser pulse duration decreases to 117 ns. Still, this pulse duration is almost 20% longer compared to other large volume KrCl lasers [15]. We have found in similar experiments that the pulse energy decreased strongly for  $R_{\text{OC}} = 0.5$  or below.

#### 4 Conclusion

We have demonstrated the first long-pulse discharge pumped high-pressure KrCl laser with a high discharge quality. The laser comprises a three-electrode pre-pulse–mainpulse circuit as pump source. The pump circuit sustains the gas discharges for 270 ns with specific pump power density of up to  $340 \text{ kW cm}^{-3}$ . Under these pump conditions, a beam divergence of smaller than 1 mrad is measured for both output beams when a plane–plane resonator is used with 10% outcoupling. A comparison with a long-pulse XeCl laser shows that the achieved discharge homogeneity is very high. Furthermore, the measurement shows that the discharge homogeneity remains high until the end of the pump pulse, as the laser pulse, used to measure the beam divergence, traverses the gain medium throughout the full pump duration. Under these circumstances, the consumption of the halogen donor is observed to be a limiting factor rather than the growth of instabilities.

The maximum laser pulse duration and energy increases when a lower Kr partial pressure of 90 mbar (instead of 130 mbar) is used. This lower Kr concentration is supposed to be favorable as the quenching of the upper state population and the halogen donor consumption slows down. The highest output energy is measured for a buffer gas pressure of 4.3 bar. Pumping the discharge under optimum conditions and using a stable resonator resulted in a maximum specific energy of 0.45 J/l with a pulse duration of 117 ns and an efficiency of 0.63%. This is an improvement of the pulse duration for these high output energies of almost 20%. The pulse duration increased for a resonator feedback of 90% to almost 150 ns with 0.27 J/l.

**ACKNOWLEDGEMENTS** The author thanks A. Azarov and D. Mathew for many helpful suggestions and discussions. This work was financially supported by SenterNovem, The Netherlands.

#### REFERENCES

- 1 D. Basting, G. Marowsky, *Excimer Laser Technology* (Springer, Berlin Heidelberg, 2005)
- 2 J.J. Ewing, *IEEE J. Sel. Top. Quantum Electron.* **6**, 1061 (2000)
- 3 S. Watanabe, A. Endoh, *Appl. Phys. Lett.* **41**, 799 (1982)
- 4 K. Miyazaki, T. Hasama, K. Yamada, T. Fukatsu, T. Eura, T. Sato, *J. Appl. Phys.* **60**, 2721 (1986)
- 5 R.S. Taylor, K.E. Leopold, *Appl. Phys. Lett.* **46**, 335 (1985)
- 6 R.S. Taylor, K.E. Leopold, *Appl. Phys. B* **59**, 479 (1994)
- 7 R.S. Taylor, K.E. Leopold, *J. Appl. Phys.* **56**, 22 (1989)
- 8 J.W. Gerritsen, A.L. Keet, G.J. Ernst, W.J. Witteman, *J. Appl. Phys.* **67**, 3517 (1990)
- 9 S. Bollanti, P. di Lazzaro, F. Flora, T. Letardi, D. Murra, C. Petrucci, O. Uteza, *Opt. Commun.* **132**, 565 (1996)
- 10 A.N. Panchenko, V.F. Tarasenko, *IEEE J. Quantum Electron.* **QE-31**, 1231 (1995)
- 11 J.-M. Hueber, B.L. Fontaine, N. Bernard, B.M. Forestier, M.L. Sentis, P.C. Delaporte, *Appl. Phys. Lett.* **62**, 2269 (1992)
- 12 M. Makarov, Y. Bychkov, *J. Phys. D Appl. Phys.* **29**, 350 (1996)
- 13 T.J. McKee, S.D. Hastie, *J. Appl. Phys.* **56**, 2170 (1984)
- 14 V.V. Borovkov, V.V. Voronin, S.L. Voronov, D.I. Zenkov, B.V. Lazhintsev, V.A. NorArevyan, V.A. Tananakin, G.I. Fedorov, I.M. Yutkin, *Quantum Electron.* **25**, 414 (1995)
- 15 V.V. Borovkov, V.V. Voronin, S.L. Voronov, D.I. Zenkov, B.V. Lazhintsev, V.A. NorArevyan, V.A. Tananakin, G.I. Fedorov, *Quantum Electron.* **26**, 39 (1996)
- 16 R.M. Hofstra, *On the Optical Performance of the Long Pulse XeCl\* Excimer Laser*, PhD thesis, University of Twente, The Netherlands (1999)
- 17 R.M. Hofstra, F.A. van Goor, W.J. Witteman, *Opt. Commun.* **144**, 43 (1997)
- 18 F.A. van Goor, M. Trentelman, J.C.M. Timmermans, W.J. Witteman, *J. Appl. Phys.* **75**, 621 (1994)
- 19 H. Hokazono, K. Midorikawa, M. Obara, T. Fujioka, *J. Appl. Phys.* **56**, 680 (1984)
- 20 V.É. Peét, E.V. Slivinskiĭ, A.B. Treshchalov, *Sov. J. Quantum Electron.* **20**, 372 (1990)